

Polaron and Exciton Delocalization in Oligomers of High-**Performance Polymer PTB7**

Jens Niklas,*^{,†} Tianyue Zheng,[‡] Andriy Neshchadin,[‡] Kristy L. Mardis,[§] Luping Yu,*,[‡] and Oleg G. Poluektov*,†

Supporting Information

ABSTRACT: A key characteristic of organic photovoltaic cells is the efficient charge separation in the active layer. Sufficient delocalization of the positive polaron in organic photovoltaics is considered essential for the effective separation of the opposite charges and the suppression of recombination. We use light-induced EPR and ENDOR spectroscopy combined with DFT calculations to determine the electronic structure of the positive polaron in PTB7-type oligomers. Utilizing the superior spectral resolution of high-frequency (130 GHz) D-band EPR, the principal components of the g tensors were determined. Pulsed ENDOR spectroscopy at X-band allowed the measurement of ¹H hyperfine coupling constants. A comparison of g tensors and ¹H hyperfine coupling constants of the PTB7-type oligomers with the high-performance PTB7 polymer revealed a delocalization of the



positive polaron in the polymer over about four monomeric units, corresponding to about 45 Å in length. Our current study thus not only determines the polaron delocalization length in PTB7 but also validates the approach combining EPR/ENDOR spectroscopy with DFT-calculated magnetic resonance parameters. This is of importance in those cases where oligomers of defined length are not easily obtained. In addition, the delocalization of the neutral triplet exciton was also determined in the oligomers and compared with polymer PTB7. The analysis revealed that the neutral triplet exciton is substantially more delocalized than the positive polaron, exceeding 10 monomeric units.

INTRODUCTION

Organic photovoltaic (OPV) cells are lightweight, flexible, and environmentally friendly and can be made of a large and constantly growing choice of organic electron donor and electron acceptor materials. 1,2 A very popular configuration for the active layer is the bulk heterojunction (BHJ), which consists of an intercalating network of electron donor and acceptor materials.3-6 Semiconducting organic polymers are the most widely used donor material. Upon light absorption by the electron donor, an excited state is generated and the exciton then migrates to the donor-acceptor interface, which is followed by electron transfer from the donor to the acceptor. The acceptor molecule was typically a fullerene derivative, but more recently polymers and especially small molecules have been very successfully developed as electron acceptors to improve organic photovoltaics. 9-17 Further successive charge-transfer steps finally result in two stable, separated ions, a positive polaron (radical cation) on the donor polymer, and a negative polaron (radical anion) on the acceptor. An important characteristic of OPV cells is efficient charge separation and suppression of recombination in the active layer. Sufficient delocalization of the positive polaron in

excitonic PVs is considered essential to achieving this. Many previous studies using a wide variety of materials and methods have attempted to determine the extent of delocalization but often yielded only qualitative information. This is frequently due to the weak dependence of the spectroscopic parameters on the actual delocalization of the positive polaron and the additional influence of the surroundings (e.g., solvent molecules) on those parameters and the necessity of certain assumptions. 18-24 In contrast, electron paramagnetic resonance (EPR) spectroscopy, preferably performed at several frequencies, and its advanced techniques such as electronnuclear double-resonance (ENDOR) and electron spin-echo envelope modulation (ESEEM) are ideally suited to study the delocalization of the positive polaron on the polymer. ^{25–30} In our previous study, the delocalization length in high-performance polymer PTB7 (and two other polymers, P3HT and PCDTBT) was indirectly deduced by a comparison of experimental ¹H hyperfine coupling constants with the ones obtained by density functional theory (DFT) calculations.²

Received: October 9, 2019 Published: December 20, 2019

1359

[†]Chemical Sciences and Engineering Division, Argonne National Laboratory, Lemont, Illinois 60439, United States

[‡]Department of Chemistry and James Franck Institute, University of Chicago, Chicago, Illinois 60637, United States

[§]Department of Chemistry, Physics, and Engineering Studies, Chicago State University, Chicago, Illinois 60628, United States

Journal of the American Chemical Society

Figure 1. Structures of the shorter PTB7-type oligomer model compounds investigated (B, benzodithiophene unit; F, fluorinated thieno[3,4-b]thiophene unit; TIPS, triisopropylsilyl; R, 2-ethylhexyl). Figure S1 shows the structures of the TIPS-BFB oligomer with alkyl side chains and the PTB7 and PTB7-Th polymers.

From the chemical/materials point of view, this approach relies only on the preparation of blends of the donor polymer with acceptors such as fullerenes and does not require potential cumbersome synthesis such as the preparation of oligomers of well-defined length or site-specific isotope labeling. This appealing combination has, despite its growing applicability, certain limitations. Among those are the inherent shortcomings of DFT as not being an ab initio method, where the choice of the functional (in particular, the fraction of exchange) influences the obtained delocalization of the positive polaron. In addition, there is also the limited accuracy of the calculation of magnetic resonance parameters even if the delocalization is properly calculated, which also depends on the chosen functional. Computational requirements restrict the size of systems which can be investigated, setting a limit to the length of the oligomers which can be calculated, requiring termination of the often-long side chains with their number of conformational substates and the extent of completeness of the basis sets. Furthermore, the polymer backbone also has a potentially large number of conformations, which have to be calculated. Independent of what computational method (DFT or higherlevel wave-function-based methods such as MP2 and coupled cluster) is used, a potentially serious issue is that the polymer environment and its distribution (its heterogeneity) cannot simply be taken into account explicitly. These are, for example, interactions with solvent/additive molecules, interaction with other polymer chains or distant parts of the same polymer chain, and twists and kinks of the polymer chains which all could substantially influence delocalization. Purely computational approaches, without experimental reference data sensitive to delocalization, tend to be even more vulnerable to the partial or substantial neglect of the environment. Hence, experiment-based direct access to the delocalization is very valuable since it not only can determine the delocalization length for one specific polymer on a purely experimental basis but also can be used to validate computational approaches not only for a specific polymer but for a whole class of polymers. Polymer PTB7 and its derivative PTB7-Th (also called PCE10 and PBDTT-FTTE; for chemical nomenclature and structural formulas, see the SI) are among the highest-performing polymers in the OPV field. 31-33 In addition, the general design principles of the PTB7 polymer class have also been used for other polymer groups. Hence, the PTB7 polymer is

ideally suited as a model for high-performing organic photovoltaic polymers.

In this work, we combine multifrequency EPR and ENDOR spectroscopy with DFT calculations to investigate the electronic structure of the positive polaron in several short PTB7-type oligomers (Figure 1). The positive polaron on PTB7-type oligomers was created by the illumination of a blend with fullerene derivative PC61BM. This way of generating the photoinduced positive polaron prevents artificial localization, such as that obtained by chemical oxidation (e.g., by treating polymer films with iodine). In the latter case, an extra localization of the positive charge due to Coulomb interaction with counterions may occur. 28,29 In addition, the EPR spectrum of the negative polaron on PC₆₁BM at high frequencies does not overlap with that of the positive polaron on PTB7-type oligomers.²⁹ The information obtained is then compared with the PTB7 polymer itself and allows a precise determination of the polaron delocalization under real-world OPV conditions. Furthermore, the delocalization of the neutral triplet exciton was also determined in these oligomers and compared with polymer PTB7.

■ RESULTS AND DISCUSSION

EPR Spectroscopy on PTB7-Type Oligomers in their Radical Cation State (Positive Polaron). The PTB7-type oligomers are prepared in a blend with fullerene derivative PC₆₁BM and illuminated with visible light at cryogenic temperatures. Light absorption is followed by fast energy and electron transfer steps which finally yield the positive polaron on the oligomer and the negative polaron on the fullerene derivative. 17,4,7 If pairs of these ions are in close proximity (e.g., next-nearest neighbors at the donor-acceptor interface), then they recombine quickly even at cryogenic temperatures. However, if the opposite charges move several tens of Angstroms away from each other, then these polarons (radical ions) are essentially stable at cryogenic temperatures and allow the application of steady state spectroscopy.³⁴ Furthermore, at these distances (>30 Å) the magnetic interactions between these species are negligible and EPR spectroscopy essentially detects the spectral signatures of isolated species. 25 At standard frequencies such as the X-band (9.5 GHz, 340 mT), the signals of the PTB7-type oligomer and polymer partially overlap with that of fullerene derivative PC₆₁BM and the g tensor of the

positive polaron is not resolved. ²⁹ It is typical for blends of organic polymers and fullerene derivatives that high-frequency/high-field EPR (\geq 95 GHz, 3.4 T) is necessary to achieve sufficient spectral resolution. ^{25,26,28,29,35} We thus used high-frequency EPR at the D-band (130 GHz, 4.6 T), where the approximately 14 times higher frequency allowed the spectral separation of PTB7-type oligomer and PC₆₁BM polaron signals and also the unambiguous determination of the PTB7-type oligomer g tensor. Figure 2 displays pulsed D-

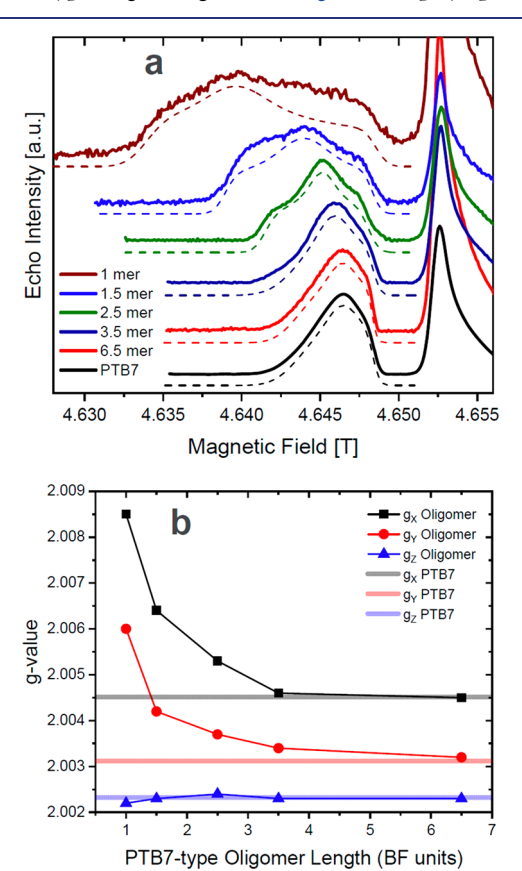


Figure 2. (a) High-frequency pulsed (130 GHz, D-band) EPR spectra of illuminated blends consisting of fullerene PC₆₁BM with PTB7-type oligomers (Figure 1) and the PTB7 polymer at cryogenic temperature. The low-field part of the spectra (<4.650 T) is due to the PTB7-type oligomers and the PTB7 polymer (positive polaron), while the high-field part (>4.650 T) is due to the negative polaron on PC₆₁BM. ^{25,26,28,29,35,36} Dashed lines are spectral simulations of the positive polaron. Simulation parameters are summarized in Table 1. (b) Principal g values of the positive polaron on the PTB7-type oligomer model compounds in comparison with the PTB7 polymer as determined by high-frequency EPR ($g_x > g_y > g_z$). The g_z axis is perpendicular to the π-system, while the g_x and g_z axes lie in the plane of the molecule (as determined by DFT calculations).

band spectra of PTB7-type oligomer blends. The low-field part of the spectra (<4.650 T) is due to the PTB7-type oligomers and the PTB7 polymer, while the high-field part (>4.650 T) is due to fullerene $PC_{61}BM$; g values and the line shape of the negative polaron on $PC_{61}BM$ are essentially identical in the different blends and are in very good agreement with previous results. ^{25,26,28,29,35,36} Hence, the following discussion focuses exclusively on the positive polaron on the PTB7-type oligomers and the PTB7 polymer.

The EPR spectra of the two shortest oligomers, the 1 mer and the 1.5 mer, exhibit a lower signal-to-noise ratio since only

a small fraction of oligomer-fullerene blends achieve stable charge separation at cryogenic temperatures. This is consistent with the lower efficiency of OPV cells based on short PTB7type oligomers. The lowest principal g value of the positive polaron, g_{zz} is essentially the same in all oligomers and polymer PTB7 and very similar to the free electron g value ($g_e \approx$ 2.0023). From previous²⁹ and current DFT calculations, it is known that this component of the g tensor is perpendicular to the π -system of all PTB7-type oligomers and the polymer and should be largely independent of the number of BF units over which the positive polaron is delocalized.^{37–39} The other two components of the g tensor $(g_x \text{ and } g_y)$ lie in the molecular plane of the oligomers and are expected to be sensitive to the polaron delocalization, which is indeed experimentally observed. The g tensors of the 1 mer, the 1.5 mer, and the 2.5 mer exhibit significant deviations from that of PTB7, while the 6.5 mer is completely in line with polymer PTB7. The delocalization length is thus clearly between 2.5 and 6.5 units. The g tensor of the 3.5 mer (TIPS-4B3F) deviates only slightly from the polymer. This leads to the conclusion that the best description for the delocalization length is about 4 BF units, complying with our previous estimate of 3 to 4 BF units using EPR/ENDOR spectroscopy on the PTB7 polymer in combination with DFT calculations. 25

Another set of magnetic resonance parameters sensitive to the delocalization of the positive polaron consists of hyperfine coupling constants, in particular, those of ¹H. In fact, in our previous study of the PTB7 polymer, the ¹H hyperfine coupling constants were better indicators of the delocalization length than the g tensor,²⁹ but the ¹H hyperfine couplings are too small to be resolved in the EPR spectra at either the Xband or D-band. Hence, X-band ENDOR spectroscopy was used to determine the hyperfine coupling constants. This type of experiment corresponds to performing an NMR experiment (driving nuclear transitions using an rf pulse) but detecting with the EPR technique (mw pulses) and is often used to increase the spectral resolution of EPR lines which are inhomogeneously broadened by hyperfine interactions. $^{40-43}$ Within a conventional oligomer extrapolation approach, 20,44-48 the largest hyperfine coupling constants should scale proportionally to 1/n, with n being the number of monomeric units (one unit consisting of one subunit B and one subunit F) over which the positive polaron is delocalized. Under our experimental conditions, the ENDOR signals of ¹H are located at $v_{RF} = v_{1H} \pm \frac{A}{2}$, with A being the hyperfine coupling constant of a particular nucleus and v_{1H} being the Larmor frequency of a "free" proton. Other nuclei with spin (beside hydrogen) are not expected to contribute substantially to the ENDOR spectra because of the combination of their smaller magnetic moment and lower abundance in the oligomer. Figure 3a shows pulsed ENDOR spectra of the positive polaron on the PTB7-type oligomers and polymer. We performed Davies-type ENDOR because it is free of blind-spot distortions for |A| > 0. The Larmor frequency of a free proton v_{1H} is about 14.8 MHz in our magnetic field (~340 mT) and can be easily recognized by the relatively narrow and intense line in the center of the spectrum. The wider the ENDOR signal, the larger the hyperfine coupling constant(s). The ENDOR spectra of the two shortest oligomers are approximately equal in width and quite noisy since only a very small fraction of oligomer-fullerene blends achieves stable charge separation, even at cryogenic temperatures (similar to

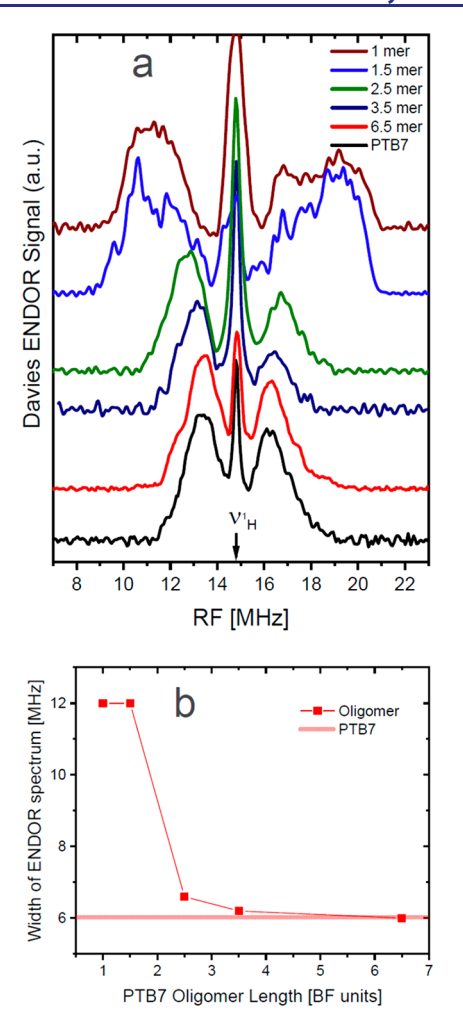


Figure 3. (a) X-band pulsed Davies ENDOR spectra of illuminated blends consisting of fullerene PC₆₁BM with PTB7-type oligomers (Figure 1) and the PTB7 polymer at cryogenic temperature. (b) Overall width of Davies ENDOR spectra for PTB7-type oligomer model compounds in comparison with the PTB7 polymer.

the EPR signals at the D-band, Figure 2). In general, the same picture is conveyed for the $^1\mathrm{H}$ hyperfine interaction as for the g tensor: 1 mer, 1.5 mer, and 2.5 mer are substantially different from the polymer, which is identical to the 6.5 mer, and the 3.5 mer is very slightly different from the polymer (Figure 3b). Thus, we can conclude that the delocalization of the positive polaron extends no further than the length of the tetramer.

EPR Spectroscopy on PTB7-Type Oligomers in the Photoexcited Triplet State. The neutral photoexcited triplet (S = 1) of the PTB7-type oligomers is another paramagnetic state and hence accessible by EPR spectroscopy. Pulsed laser irradiation of the oligomers generates an excited singlet state, which can be converted with a certain yield to the triplet state by the intersystem crossing (ISC) process. The interactions between two spins within a triplet state are characterized by the zero-field splitting (ZFS) parameter D, which is determined by the overlap of the wave functions between these two electrons. 49,50 Thus, the magnitude, |D|, will be larger when the two unpaired electrons are closer. A larger |D| will result in a wider spectrum. Increasing delocalization of the triplet exciton in larger oligomers should decrease |D| and make the spectrum narrower. This is qualitatively somewhat similar to the ENDOR results for the positive polaron

discussed above. Note that while this highly simplified approach can be an appropriate approximation in these oligomers, it must be taken with great care when dealing with other geometries. ⁵¹ Figure 4a shows the X-band spectra of

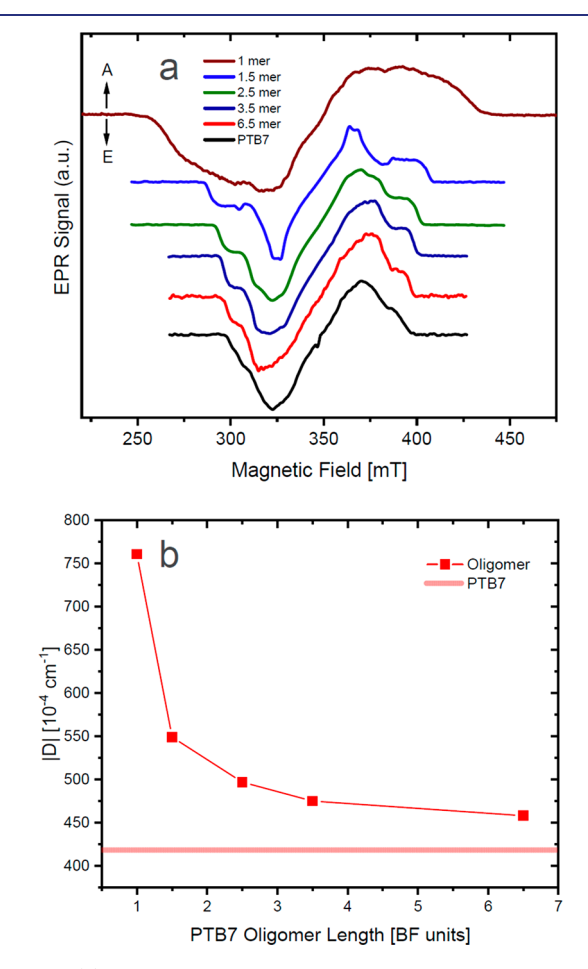


Figure 4. (a) Transient X-band EPR spectra of PTB7-type oligomers in their neutral photoexcited triplet state at cryogenic temperature. The integration after the laser flash is 250-1250 ns. Positive signals correspond to absorption (*A*), and negative signals correspond to emission (*E*). (b) Magnitude of ZFS parameter D (|D|) for PTB7-type oligomer model compounds in comparison with the PTB7 polymer.

the triplet state in the PTB7-type oligomers and polymer. While a decrease in |D| is indeed observed with increasing oligomer length, the spectrum of the 6.5 mer is clearly not yet identical to that of the polymer, indicating that the triplet exciton is substantially more delocalized (Figure 4b). Extrapolation from the data for the 1.5 mer, 2.5 mer, 3.5 mer, and 6.5 mer suggests that it is even delocalized over more than 10 BF units. Hence, we can safely conclude that the neutral triplet exciton on PTB7 is substantially more delocalized than the positive polaron counterpart.

This is an important discovery, considering the number of publications which claim the high localization of triplet excitons in metalorganic oligomers and polymers. $^{18,22-24}$ However, systematic data on the delocalization of the triplet exciton in pure organic conjugated systems are not available because triplet states are spectroscopically "silent" as a result of the forbidden character of the S_0-T_1 transition and the low sensitivity of the energetic parameters of the triplet exciton with respect to the length of the oligomer. 18,24 While multiple

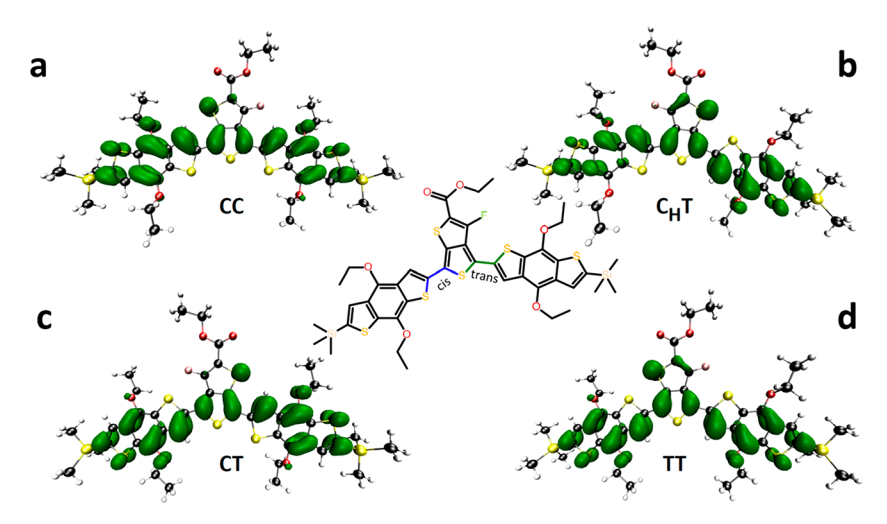


Figure 5. PBEh-3c-optimized structures of the PTB7-type n=1.5 oligomer cation radical (positive polaron). All ethylhexyl groups were replaced with ethyl groups. Structures are very similar for other functionals. The conformations are defined by the relative positions of the sulfur atoms as shown on inset where the blue highlighted bond is labeled cis/C; the green trans/T. Due to symmetry of the molecule, the CT structure (c) could also be referred to as TC. However, there is a potential F–H bond in structure C_HT (b). Note, that structures (b) and (c) are shown in a different orientation than the others for better visual presentation. Spin density calculations with the B3LYP||EPRII basis and def2-tzvpp basis for S and Si atoms. The spin density isosurface is shown at 0.001 e/a_0^3 . (a) CC, (b) C_HT , (c) CT, and (d) TT.

Table 1. Experimental g Values and Width of the Pulsed ¹H ENDOR Spectrum for Positive Polarons and ZFS Parameters for Triplet Exciton on the PTB7-Type Oligomers and PTB7 Polymer

	1 mer	1.5 mer	2.5 mer	3.5 mer	6.5 mer	PTB7
g_z	2.0022	2.0023	2.0024	2.0023	2.0023	2.0023
g_y	2.0060	2.0042	2.0037	2.0034	2.0032	2.0031
g_x	2.0085	2.0064	2.0053	2.0046	2.0045	2.0045
width of ¹ H ENDOR spectrum [MHz]	~12	~12	6.6	6.2	6.0	6.0
ZFS parameters D , E [10 ⁻⁴ cm ⁻¹]	761, 138	549, 64	497, 57	475, 56	458, 70	417, 56

Table 2. Effect of Conformation on g Values for the n = 1.5 Oligomer Conformers^a

	B3LYP 6-31G*				PBEh-3clldef2-mSVP				
g	TT (1.0)	CT (0.8)	$C_{H}T$ (0.0)	CC (0.2)	TT (0.0)	CT (0.4)	C _H T (2.1)	CC (0.6)	exptl
g_z	2.0022	2.0022	2.0022	2.0022	2.0022	2.0022	2.0020	2.0022	2.0023
g_y	2.0039	2.0043	2.0041	2.0040	2.0042	2.0044	2.0037	2.0042	2.0042
g_x	2.0060	2.0050	2.0059	2.0050	2.0058	2.0050	2.0057	2.0052	2.0064

"Optimizations are from the B3LYPll6-31G* and PBEh-3clldef2-mSVP methods, and all g values were calculated using the B3LYPllEPRII basis and def2-tzvpp basis for S and Si atoms. "Conformations are defined as cis/trans (C/T) as shown in Figure 5. Parentheses contain energies in kcal/mol.

cases for a metalorganic system are facilitated by efficient ISC, induced by heavy metal ions, these systems cannot be directly compared with pure organic conjugated oligomers. Thus, in ref 20 the experimental data on T_1 – S_0 energies of oligofluorenes clearly demonstrate that the triplet exciton might be delocalized over more than 10 repeating units. Hence we conclude, that the delocalization of triplet excitons is not well understood and requires further investigation.

DFT Calculations. With the experimental *g* tensor and hyperfine tensors for a variety of PTB7-type oligomers now available as reference, density functional theory (DFT) calculations were performed to better understand the electronic properties of these oligomers. The calculations can provide information such as the energies and thus probabilities of the various potential conformers and the distribution of the unpaired spin density in the positive polaron/radical cation (charge +1) over the oligomers. This information is not available from the experimental data. In return, experimentally obtained magnetic resonance parameters such as *g* values and

hyperfine coupling constants can be directly compared with the calculated ones and thus act as a control if the structural models (such as the conformation and terminated side chains) and computational level (functional, basis sets, etc.) are chosen appropriately. The g tensor and hyperfine calculations of such molecules are typically quite successful, yielding good agreement with experimental data. DFT modeling shows that conformers with similar energies (accessible at ambient temperature) exist in this type of molecule, as was shown previously.²⁹ While the B and F subunits (Figure 1) themselves are very stable, rotations are possible around the bonds connecting them with rotational barriers of 11 to 12 kcal/mol for the charged species and 3.5 kcal/mol for the neutral species (Figure S3), and the stable conformers take either the cis or the trans configuration (abbreviated C and T in the following text, respectively; see Figure 5).

Figure 5 shows the optimized structures and spin densities of all conformations of the 1.5 mer, with Table 2 summarizing the calculated principal g values for all possible conformations.

The spin density plots show significant spin density only on the backbone but not on the fluorine atom or the alkyl or silicon groups. The termination of the alkyl and isopropyl groups had only very small effects on the *g* values (Table S2).

The g_z value is essentially invariant with respect to the conformation and complies with the experimentally determined value. It can thus not be used to distinguish between different conformers. The g_y value changes by up to 5×10^{-4} depending on the conformation, and the g_x value changes by up to 1×10^{-3} , which indicates that the latter is a better indicator for the respective conformer. These results indicate that the CC and CT conformers are most likely not present under our experimental conditions.

Further calculations were performed for all possible conformers of the PTB7-type oligomer with n=2.5. Functionals PBEh-3clldef2-mSVP and ω B97XD3ll6-31G* were used (Table S10). A complete computational study of the PTB7-type oligomers including those larger than n=2.5 is significantly more challenging and will require significant computational resources.

CONCLUSIONS

We have carried out a comprehensive EPR and DFT study of the characteristic EPR parameters of the positive polaron/ cation radical of PTB7-type oligomers. A comparison of the g tensors and ¹H hyperfine couplings of the PTB7 oligomers with the polymer revealed a delocalization of the positive polaron about four monomeric units, corresponding to about 45 Å on the polymer chain. The delocalization length derived from this study is in excellent agreement with our previous EPR and ENDOR study of polymer PTB7, where the delocalization length was indirectly derived from a comparison of the experimental and calculated ¹H hyperfine couplings. The experimental results obtained for the shortest oligomers have been compared with DFT calculations, which show good agreement with the selected conformations of the oligomer. Our current study thus not only determines the polaron delocalization length in PTB7 but also validates the approach combining EPR/ENDOR with calculated magnetic resonance parameters. In addition, the delocalization of the neutral triplet exciton in the oligomers was also determined and compared with polymer PTB7. The analysis revealed that the neutral triplet exciton is substantially more delocalized than the positive polaron, exceeding 10 monomeric units. This work clearly demonstrates that EPR spectroscopy in combination with DFT is a powerful approach for investigating the electronic structure of paramagnetic organic molecules and its interactions with the solid-state environment.

■ EXPERIMENTAL SECTION

Sample Preparation. Organic polymer PTB7 and its oligomers were synthesized as described previously. 31,32,52,53 Soluble fullerene derivative C_{60} -PCBM (P C_{61} BM) was obtained from Sigma-Aldrich (St. Louis, MO). Polymer/oligomer—fullerene mixtures (1:2 or 1:4 weight ratios) were prepared under anaerobic conditions in a N_2 drybox using deoxygenated toluene or chlorobenzene as the solvent (Sigma-Aldrich). The concentrations of the solutions were in the 5–15 mg/mL range. Samples for triplet EPR spectroscopy contained no fullerenes. The solutions were used to fill EPR quartz tubes, which were sealed under a N_2 atmosphere, and then were frozen quickly in liquid nitrogen. Measurements were performed at cryogenic temperatures to minimize light-induced degradation (photodamage) of the samples.

EPR Spectroscopy. Continuous wave (cw) X-band (9 to 10 GHz) EPR experiments were carried out with Bruker ELEXSYS E580 and ELEXSYS E500 II EPR spectrometers (Bruker Biospin, Rheinstetten, Germany) equipped with a Bruker ER4102ST resonator or a Flexline dielectric ring resonator (Bruker EN 4118X-MD4-W1). Pulsed EPR and pulsed ENDOR experiments were performed on the ELEXSYS E580 spectrometer using a BT01000-AlphaSA 1 kW rf amplifier (TOMCO Technologies, Stepney, Australia). ENDOR spectra $^{40-42}$ were recorded using (i) the Davies ENDOR sequence (π -t- π /2- τ - π - τ -echo) with an inversion π -pulse of 148 ns, t = 10 μ s, and an rf π -pulse of 6 μ s or (ii) the Mims ENDOR sequence (π /2- τ - π /2- τ -echo) with a π /2 pulse of 24 ns, t = 10 μ s, and an rf π -pulse of 6 μ s.

Helium gas-flow cryostats (Oxford Instruments and ICE Oxford, U.K.) and an ITC (Oxford Instruments, U.K.) were used for cryogenic temperatures.

Light excitation was carried out directly in the resonator with 532 nm laser light (Nd:YAG Laser, INDI, Newport) or with a white-light LED (Thorlabs, Newton).

High-frequency (hf) EPR measurements were performed on a home-built D-band (130 GHz) spectrometer equipped with a single-mode TE_{011} cylindrical cavity. S4,55 D-band EPR spectra were recorded in pulse mode in order to remove the microwave phase distortion due to fast-passage effects at low temperatures. Light excitation was carried out directly in the cavity of the spectrometer with 532 nm laser light through an optical fiber (Nd:YAG Laser, INDI, Newport). Data processing was carried out using Xepr (Bruker BioSpin, Rheinstetten) and MatlabTM 7.11.2 (MathWorks, Natick) environment. Simulations of the EPR spectra were performed using the EasySpin software package. S6

Density Functional Theory Calculations. Initial structures were built in PQSMOL. The initial geometry optimizations were carried out using density functional theory (DFT) and the B3LYP functional \$57-60 using, successively, the 6-31G and the 6-31G+(d) basis sets as implemented in PQSMol. 61 Frequency calculations in PQSMOL were performed on all n = 1.5 optimized structures to ensure that stable minima were obtained. All additional optimized structures using alternate functionals (PBEh-3c, B9703c, wB97X-D3, etc.) were obtained using program package ORCA (v. 4.0.0.2)⁶² with the B3LYP-optimized structures as starting points. Orca 4.1.1 was used to obtain the spectroscopic parameters for each structure via single-point DFT calculations, with the B3LYP functional in combination with the EPRII basis set^{63,64} for the C, H, and O atoms and the def2-TZVPP basis set for the S and Si atoms. The principal electronic g values were calculated by employing the coupled-perturbed Kohn-Sham equations and the spin-orbit operator computed using the RI approximation for the Coulombic term and the one-center approximation for the exchange term (SOMF(1X)).

ASSOCIATED CONTENT

S Supporting Information

The Supporting Information is available free of charge at https://pubs.acs.org/doi/10.1021/jacs.9b10859.

Effects of functional and basis set on the calculated energies, g values, and hyperfine coupling (PDF)

AUTHOR INFORMATION

Corresponding Authors

*E-mail: jniklas@anl.gov.

*E-mail: lupingyu@uchicago.edu.

*E-mail: oleg@anl.gov.

ORCID ®

Jens Niklas: 0000-0002-6462-2680 Kristy L. Mardis: 0000-0003-2633-9304 Oleg G. Poluektov: 0000-0003-3067-9272

Notes

The authors declare no competing financial interest.

ACKNOWLEDGMENTS

The experimental part is based upon work supported by the U.S. Department of Energy, Office of Science, Office of Basic Energy Sciences, Division of Chemical Sciences, Geosciences, and Biosciences under contract number DE-AC02-06CH11357 at Argonne National Laboratory. This work was supported by the NSF (Chem-1802274, LPY) and partially supported by the University of Chicago Materials Research Science and Engineering Center, which is funded by the National Science Foundation under award number DMR-1420709. We gratefully acknowledge the computing resources provided on Blues and Bebop, high-performance computing clusters operated by the Laboratory Computing Resource Center at Argonne National Laboratory. The computational work was supported by the Illinois Space Grant Consortium and the National Institutes of Health (SC3 GM122614).

REFERENCES

- (1) Brabec, C. J., Scherf, U., Dyakonov, V., Eds.; Organic Photovoltaics: Materials, Device Physics, and Manufacturing Technologies, 2nd ed.; Wiley-VCH: Weinheim, Germany, 2014.
- (2) Inganas, O. Organic Photovoltaics over Three Decades. Adv. Mater. 2018, 30, 1800388.
- (3) Yu, G.; Gao, J.; Hummelen, J. C.; Wudl, F.; Heeger, A. J. Polymer Photovoltaic Cells - Enhanced Efficiencies Via a Network of Internal Donor-Acceptor Heterojunctions. Science 1995, 270, 1789-
- (4) Deibel, C.; Dyakonov, V. Polymer-Fullerene Bulk Heterojunction Solar Cells. Rep. Prog. Phys. 2010, 73, 096401.
- (5) Lee, H.; Park, C.; Sin, D. H.; Park, J. H.; Cho, K. Recent Advances in Morphology Optimization for Organic Photovoltaics. Adv. Mater. 2018, 30, 1800453.
- (6) Lu, L. Y.; Zheng, T. Y.; Wu, Q. H.; Schneider, A. M.; Zhao, D. L.; Yu, L. P. Recent Advances in Bulk Heterojunction Polymer Solar Cells. Chem. Rev. 2015, 115, 12666-12731.
- (7) Clarke, T. M.; Durrant, J. R. Charge Photogeneration in Organic Solar Cells. Chem. Rev. 2010, 110, 6736-6767.
- (8) Laquai, F.; Andrienko, D.; Deibel, C.; Neher, D. Charge Carrier Generation, Recombination, and Extraction in Polymer-Fullerene Bulk Heterojunction Organic Solar Cells. In Elementary Processes in Organic Photovoltaics; Leo, K., Ed.; Springer-Verlag: Berlin, 2017; Vol. 272, pp 267-291.
- (9) Hou, J. H.; Inganas, O.; Friend, R. H.; Gao, F. Organic solar cells based on non-fullerene acceptors. Nat. Mater. 2018, 17, 119-128.
- (10) Zhang, G. Y.; Zhao, J. B.; Chow, P. C. Y.; Jiang, K.; Zhang, J. Q.; Zhu, Z. L.; Zhang, J.; Huang, F.; Yan, H. Nonfullerene Acceptor Molecules for Bulk Heterojunction Organic Solar Cells. Chem. Rev. 2018, 118, 3447-3507.
- (11) Facchetti, A. Polymeric Acceptor Semiconductors for Organic Solar Cells. Organic Photovoltaics; Wiley-VCH Verlag: 2014; pp 239-
- (12) Wang, G.; Melkonyan, F. S.; Facchetti, A.; Marks, T. J. All-Polymer Solar Cells: Recent Progress, Challenges, and Prospects. Angew. Chem., Int. Ed. 2019, 58, 4129-4142.
- (13) Lu, L.; Kelly, M. A.; You, W.; Yu, L. Status and prospects for ternary organic photovoltaics. Nat. Photonics 2015, 9, 491.
- (14) Yuan, J.; Zhang, Y.; Zhou, L.; Zhang, G.; Yip, H.-L.; Lau, T.-K.; Lu, X.; Zhu, C.; Peng, H.; Johnson, P. A.; Leclerc, M.; Cao, Y.; Ulanski, J.; Li, Y.; Zou, Y. Single-Junction Organic Solar Cell with over 15% Efficiency Using Fused-Ring Acceptor with Electron-Deficient Core. Joule 2019, 3, 1140-1151.
- (15) Cui, Y.; Yao, H.; Zhang, J.; Zhang, T.; Wang, Y.; Hong, L.; Xian, K.; Xu, B.; Zhang, S.; Peng, J.; Wei, Z.; Gao, F.; Hou, J. Over 16% efficiency organic photovoltaic cells enabled by a chlorinated

- acceptor with increased open-circuit voltages. Nat. Commun. 2019, 10, 2515.
- (16) Wadsworth, A.; Moser, M.; Marks, A.; Little, M. S.; Gasparini, N.; Brabec, C. J.; Baran, D.; McCulloch, I. Critical review of the molecular design progress in non-fullerene electron acceptors towards commercially viable organic solar cells. Chem. Soc. Rev. 2019, 48,
- (17) Nielsen, C. B.; Holliday, S.; Chen, H. Y.; Cryer, S. J.; McCulloch, I. Non-Fullerene Electron Acceptors for Use in Organic Solar Cells. Acc. Chem. Res. 2015, 48, 2803-2812.
- (18) Beljonne, D.; Wittmann, H. F.; Kohler, A.; Graham, S.; Younus, M.; Lewis, J.; Raithby, P. R.; Khan, M. S.; Friend, R. H.; Bredas, J. L. Spatial extent of the singlet and triplet excitons in transition metalcontaining poly-ynes. J. Chem. Phys. 1996, 105, 3868-3877.
- (19) Takeda, N.; Miller, J. R. Poly(3-decylthiophene) Radical Anions and Cations in Solution: Single and Multiple Polarons and Their Delocalization Lengths in Conjugated Polymers. J. Phys. Chem. B 2012, 116, 14715-14723.
- (20) Jansson, E.; Jha, P. C.; Aren, H. Chain length dependence of singlet and triplet excited states of oligofluorenes: A density functional study. Chem. Phys. 2007, 336, 91-98.
- (21) Wasserberg, D.; Dudek, S. P.; Meskers, S. C. J.; Janssen, R. A. J. Comparison of the chain length dependence of the singlet- and triplet-excited states of oligofluorenes. Chem. Phys. Lett. 2005, 411, 273-277.
- (22) Kohler, A.; Wilson, J. S.; Friend, R. H.; Al-Suti, M. K.; Khan, M. S.; Gerhard, A.; Bassler, H. The singlet-triplet energy gap in organic and Pt-containing phenylene ethynylene polymers and monomers. J. Chem. Phys. 2002, 116, 9457-9463.
- (23) Glusac, K.; Kose, M. E.; Jiang, H.; Schanze, K. S. Triplet excited state in platinum-acetylide oligomers: Triplet localization and effects of conformation. J. Phys. Chem. B 2007, 111, 929-940.
- (24) Liu, Y.; Jiang, S. J.; Glusac, K.; Powell, D. H.; Anderson, D. F.; Schanze, K. S. Photophysics of monodisperse platinum-acetylide oligomers: Delocalization in the singlet and triplet excited states. J. Am. Chem. Soc. 2002, 124, 12412-12413.
- (25) Niklas, J.; Poluektov, O. G. Charge Transfer Processes in OPV Materials as Revealed by EPR Spectroscopy. Adv. Energy Mater. 2017, 7, 1602226.
- (26) De Ceuster, J.; Goovaerts, E.; Bouwen, A.; Hummelen, J. C.; Dyakonov, V. High-frequency (95 GHz) Electron Paramagnetic Resonance Study of the Photoinduced Charge Transfer in Conjugated Polymer-Fullerene Composites. Phys. Rev. B: Condens. Matter Mater. Phys. 2001, 64, 195206.
- (27) Dyakonov, V.; Zoriniants, G.; Scharber, M.; Brabec, C. J.; Janssen, R. A. J.; Hummelen, J. C.; Sariciftci, N. S. Photoinduced charge carriers in conjugated polymer-fullerene composites studied with light-induced electron-spin resonance. Phys. Rev. B: Condens. Matter Mater. Phys. 1999, 59, 8019-8025.
- (28) Aguirre, A.; Gast, P.; Orlinskii, S.; Akimoto, I.; Groenen, E. J. J.; El Mkami, H.; Goovaerts, E.; Van Doorslaer, S. Multifrequency EPR Analysis of the Positive Polaron in I₂-doped Poly(3-hexylthiophene) and in Poly[2-methoxy-5-(3,7-dimethyloctyloxy)]-1,4-phenylenevinylene. Phys. Chem. Chem. Phys. 2008, 10, 7129-7138.
- (29) Niklas, J.; Mardis, K. L.; Banks, B. P.; Grooms, G. M.; Sperlich, A.; Dyakonov, V.; Beaupre, S.; Leclerc, M.; Xu, T.; Yu, L.; Poluektov, O. G. Highly-Efficient Charge Separation and Polaron Delocalization in Polymer-Fullerene Bulk-Heterojunctions: A Comparative Multi-Frequency EPR and DFT Study. Phys. Chem. Chem. Phys. 2013, 15, 9562-9574.
- (30) Kuroda, S.; Marumoto, K.; Sakanaka, T.; Takeuchi, N.; Shimoi, Y.; Abe, S.; Kokubo, H.; Yamamoto, T. Electron-nuclear doubleresonance observation of spatial extent of polarons in polythiophene and poly(3-alkylthiophene). Chem. Phys. Lett. 2007, 435, 273-277.
- (31) Liang, Y. Y.; Xu, Z.; Xia, J. B.; Tsai, S. T.; Wu, Y.; Li, G.; Ray, C.; Yu, L. P. For the Bright Future-Bulk Heterojunction Polymer Solar Cells with Power Conversion Efficiency of 7.4%. Adv. Mater. 2010, 22, E135-E138.

- (32) Liang, Y. Y.; Yu, L. P. A New Class of Semiconducting Polymers for Bulk Heterojunction Solar Cells with Exceptionally High Performance. *Acc. Chem. Res.* **2010**, *43*, 1227–1236.
- (33) Cui, Y.; Yang, C. Y.; Yao, H. F.; Zhu, J.; Wang, Y. M.; Jia, G. X.; Gao, F.; Hou, J. H. Efficient Semitransparent Organic Solar Cells with Tunable Color enabled by an Ultralow-Bandgap Nonfullerene Acceptor. *Adv. Mater.* **2017**, *29*, 1703080.
- (34) Barker, A. J.; Chen, K.; Hodgkiss, J. M. Distance Distributions of Photogenerated Charge Pairs in Organic Photovoltaic Cells. *J. Am. Chem. Soc.* **2014**, *136*, 12018–12026.
- (35) Poluektov, O. G.; Filippone, S.; Martin, N.; Sperlich, A.; Deibel, C.; Dyakonov, V. Spin Signatures of Photogenerated Radical Anions in Polymer-[70]Fullerene Bulk Heterojunctions: High Frequency Pulsed EPR Spectroscopy. *J. Phys. Chem. B* **2010**, *114*, 14426–14429.
- (36) Mardis, K. L.; Webb, J. N.; Holloway, T.; Niklas, J.; Poluektov, O. G. Electronic Structure of Fullerene Acceptors in Organic Bulk-Heterojunctions: A Combined EPR and DFT Study. *J. Phys. Chem. Lett.* **2015**, *6*, 4730–4735.
- (37) Stone, A. J. g tensors of aromatic hydrocarbons. *Mol. Phys.* **1964**, 7, 311-316.
- (38) Stone, A. J. Gauge Invariance of g-Tensor. *Proc. Royal Soc. A* **1963**, 271, 424-424.
- (39) Stone, A. J. g factors of aromatic free radicals. *Mol. Phys.* **1963**, 6, 509–515.
- (40) Davies, E. R. A New Pulse ENDOR Technique. *Phys. Lett. A* **1974**, 47A, 1–2.
- (41) Mims, W. B. Pulsed ENDOR Experiments. *Proc. Royal Soc. A* **1965**, 283, 452–457.
- (42) Gemperle, C.; Schweiger, A. Pulsed Electron-Nuclear Double Resonance Methodology. *Chem. Rev.* **1991**, *91*, 1481–1505.
- (43) Schweiger, A.; Jeschke, G. Principles of Pulse Electron Paramagnetic Resonance; Oxford University Press: New York, 2001.
- (44) Bennati, M.; Grupp, A.; Mehring, M.; Bauerle, P. Pulsed EPR spectroscopy of the photoexcited triplet states of thiophene oligomers in frozen solution. *J. Phys. Chem.* **1996**, *100*, 2849–2853.
- (45) Hutchison, G. R.; Zhao, Y. J.; Delley, B.; Freeman, A. J.; Ratner, M. A.; Marks, T. J. Electronic structure of conducting polymers: Limitations of oligomer extrapolation approximations and effects of heteroatoms. *Phys. Rev. B: Condens. Matter Mater. Phys.* **2003**, *68*, 035204.
- (46) Rissler, J. Effective conjugation length of pi-conjugated systems. *Chem. Phys. Lett.* **2004**, *395*, 92–96.
- (47) Meier, H.; Stalmach, U.; Kolshorn, H. Effective conjugation length and UV/vis spectra of oligomers. *Acta Polym.* **1997**, *48*, 379–384.
- (48) Chen, H. C.; Sreearunothai, P.; Cook, A. R.; Asaoka, S.; Wu, Q.; Miller, J. R. Chain Length Dependence of Energies of Electron and Triplet Polarons in Oligofluorenes. *J. Phys. Chem. C* **2017**, *121*, 5959–5967.
- (49) Carrington, A.; McLachlan, A. D. Introduction to Magnetic Resonance; Harper & Row: New York, 1969.
- (50) Weil, J. A.; Bolton, J. R.; Weil, J. A.; Bolton, J. R.; Wertz, J. E. Electron Paramagnetic Resonance: Elementary Theory and Practical Applications; John Wiley & Sons: New York, 2007.
- (51) Richert, S.; Tait, C. E.; Timmel, C. R. Delocalisation of photoexcited triplet states probed by transient EPR and hyperfine spectroscopy. *J. Magn. Reson.* **2017**, *280*, 103–116.
- (52) Liang, Y. Y.; Wu, Y.; Feng, D. Q.; Tsai, S. T.; Son, H. J.; Li, G.; Yu, L. P. Development of New Semiconducting Polymers for High Performance Solar Cells. *J. Am. Chem. Soc.* **2009**, *131*, 56–57.
- (53) Fauvell, T. J.; Zheng, T.; Jackson, N. E.; Ratner, M. A.; Yu, L.; Chen, L. X. Photophysical and Morphological Implications of Single-Strand Conjugated Polymer Folding in Solution. *Chem. Mater.* **2016**, 28, 2814–2822.
- (54) Bresgunov, A. Y.; Dubinskii, A. A.; Krimov, V. N.; Petrov, Y. G.; Poluektov, O. G.; Lebedev, Y. S. Pulsed EPR in 2-mm Band. *Appl. Magn. Reson.* **1991**, *2*, 715–728.
- (\$\$) Poluektov, O. G.; Utschig, L. M.; Schlesselman, S. L.; Lakshmi, K. V.; Brudvig, G. W.; Kothe, G.; Thurnauer, M. C. Electronic

- Structure of the P₇₀₀ Special Pair from High-Frequency Electron Paramagnetic Resonance Spectroscopy. *J. Phys. Chem. B* **2002**, *106*, 8911–8916.
- (56) Stoll, S.; Schweiger, A. EasySpin, a Comprehensive Software Package for Spectral Simulation and Analysis in EPR. *J. Magn. Reson.* **2006**, *178*, 42–55.
- (57) Stephens, P. J.; Devlin, F. J.; Chabalowski, C. F.; Frisch, M. J. Ab Initio Calculation of Vibrational Absorption and Circular Dichroism Spectra Using Density Functional Force Fields. *J. Phys. Chem.* **1994**, 98, 11623–11627.
- (58) Becke, A. D. Density-Functional Thermochemistry. III. The Role of Exact Exchange. *J. Chem. Phys.* **1993**, *98*, 5648–5652.
- (59) Vosko, S. H.; Wilk, L.; Nusair, M. Accurate Spin-Dependent Electron Liquid Correlation Energies for Local Spin Density Calculations: a Critical Analysis. *Can. J. Phys.* **1980**, *58*, 1200–1211.
- (60) Lee, C. T.; Yang, W. T.; Parr, R. G. Development of the Colle-Salvetti Correlation-Energy Formula into a Functional of the Electron Density. *Phys. Rev. B: Condens. Matter Mater. Phys.* **1988**, *37*, 785–789.
- (61) Baker, J.; Wolinski, K.; Malagoli, M.; Kinghorn, D.; Wolinski, P.; Magyarfalvi, G.; Saebo, S.; Janowski, T.; Pulay, P. Quantum Chemistry in Parallel with PQS. J. Comput. Chem. 2009, 30, 317–335. (62) Neese, F. The ORCA Program System. WIREs Comput. Mol. Sci. 2012, 2, 73–78.
- (63) Rega, N.; Cossi, M.; Barone, V. Development and Validation of Reliable Quantum Mechanical Approaches for the Study of Free Radicals in Solution. *J. Chem. Phys.* **1996**, *105*, 11060–11067.
- (64) Barone, V. Structure, Magnetic Properties and Reactivities of Open-Shell Species from Density Functional and Self-Consistent Hybrid Methods. In *Recent Advances in Density Functional Methods (Part 1)*, Chong, D. P., (Ed.) World Scientific: Singapore, 1995; pp 287–334.
- (65) Neese, F. Efficient and Accurate Approximations to the Molecular Spin-Orbit Coupling Operator and their Use in Molecular g-Tensor Calculations. *J. Chem. Phys.* **2005**, *122*, 034107.